division of technology for society

netherlands organization for applied scientific research

STUDIES OF THE WAKE STRUCTURE OF MODEL WIND TURBINE GENERATORS

Ъу

ir. P.E.J. Vermeulen

ST BIBL.

Department of Fluid Flow Technology TNO-Apeldoorn

organization for industrial research

p.o. box 342 7300 AH apeldoorn

address laan van westenenk 501

telex 49095 tnoap phone 055 - 77 33 44

Ref. nr.: 79-012904

File nr. : 8710-8120

Date : November 1979

"Client is referred to the General Conditions for the Acceptance of Assignments of TNO with regard to his rights and duties concerning the contents of this report".

No part of this report may be reproduced in any form, by print, photoprint, microfilm or any other means without prior written permission from TNO.

TNO accepts no liability whatsoever with regard to the contents and/or the form of this report.

	CONTENTS	Page
	NOTATION	3
	1. INTRODUCTION	4
	2. EXPERIMENTAL APPARATUS AND PROGRAM	5
	3. RESULTS AND DISCUSSION	7
	3.1 Horizontal-axis wind turbine	7
	3.2 Vertical axis wind turbine	9
	4. EMPIRICAL WAKE MODEL	14
1	5. CONCLUSIONS	18
1	REFERENCES	19
u .	5 TABLES	
	19 FIGURES	

wake half width

NOTATION

C _p	power coefficient
$c_{\mathrm{T}}^{\mathrm{r}}$	drag coefficient
ď	rate of decay of centerline velocity difference
D	diameter
L ₁₁ (X)	macroscale of longitudinal fluctuations in X-direction
L _u (Y)	и и и и у- и
P	pressure
r†	dimensional cross-wind coordinate Y/R
R	turbine radius
T	drag/thrust
u'	standard deviation of longitudinal velocity fluctuations
U	mean velocity
Uo	centerline velocity difference
v'	standard deviation of lateral velocity fluctuations
X	downstream distance
X _{N.W}	length of near-wake region
Y	cross-wind coordinate
λ	tip-speed ratio
ρ	density

Subcripts

∞ undisturbed

1. INTRODUCTION

Within the first and second phases of the Dutch National Research Program on Wind Energy wind tunnel investigations have been carried out on the wake structure of wind turbine generators. These investigations have been reported by Boschloo (1) and Vermeulen (2), who studied the wake of a Vertical Axisand a Horizontal Axis Wind Turbine, respectively.

It appeared, however, necessary to conduct additional measurements in order to clarify several questions which emerged during other studies.

These additional measurements are described in this report. Also a summary of the data obtained in the first and second phase of the National Program is given.

2. EXPERIMENTAL APPARATUS AND PROGRAM

The model wind turbines were the same as described in refs. 1 and 2, having the following characteristics:

Darrieus wind turbine

number of blades 2
chord 10 mm
diameter 200 mm

blade profile DVL 00009-1.150

Horizontal-axis wind turbine

number of blades 2
chord 20 mm
diameter 360 mm
pitch 6.5 degrees
blade profile Gö-804

Wake surveys were carried out in the PIA Windtunnel of TNO-Apeldoorn as depicted in Fig. 1. Figs. 2 and 3 show both models in position. In front of the test section various turbulence grids or turbulence reducing gauzes can be placed. Within the program three different flow types have been used with the following properties:

Case 1 shear flow with $\frac{u'}{U}=3.5\%$ $L_{u}(X)\approx 30 \text{ cm}$ Case 2 shear flow with $\frac{u'}{U}$ decaying from 7% till 4% $L_{u}(X)\approx 20 \text{ cm}$ Case 3 uniform flow with $\frac{u'}{U}=1\%$ $\frac{v'}{U}=1.5\%$ $L_{u}(X)=11 \text{ cm}$ $L_{u}(Y)=8 \text{ cm}$

A more detailed description of these flows is given in lit. 2. Only case 3 is used for the present measurements.

The data aquisition system described in lit. 2 was also used for this study, comprising pitot tubes and hot-wire anemometry.

Drag measurements for the horizontal-axis machine were carried out using a drag balance instrumented with strain gauges. This balance was placed between the generator and the support structure. The additional measurements described in this report consisted of

- Horizontal-axis wind turbine
 - drag measurements to obtain the $C_{\mbox{\scriptsize T}}^{}\!\!-\!\!\lambda$ curve
 - hot-wire surveys to study the position of the tip vortices
 - static pressure measurements in the wake in order to evaluate the contribution of the pressure term in the axial momentum equation
- Vertical-axis wind turbine
 - pitot tube traverses through the wake for various tip-speed ratios

The resulting data, together with a summary of previous results, are presented in par. 3.

3. RESULTS AND DISCUSSION

3.1 Horizontal-axis wind turbine

mean velocities

Detailed mean velocity surveys have been described and discussed in ref. 2. Measured cross-wind profiles are summarized in Table 1. Tables 2 and 3 contain velocity defects measured at the wake centerline. Fig. 4 shows the effect of turbulence and tip-speed ratio on the centerline velocity defect.

momentum balance

The momentum balance for the axial direction shows that the turbine drag $^{\rm C}_{\rm T}$ instead of the power $^{\rm C}_{\rm p}$ controls the value of the total velocity defect in the wake.

The exact value of the turbine drag is therefore of primary importance for the analysis of wind-turbine wakes.

Its value can be obtained by directly integrating the momentum deficit in the wake at larger distances. Close to the wind turbine also the pressure disturbance and the turbulence contribute to the momentum balance.

In order to clarify this point it was decided to measure both the static pressure and mean velocity profiles behind the turbine and the turbine drag using a balance.

The drag-balance results are depicted in Fig. 5, together with the C_p -values which were determined previously (ref. 2).

It is found that the drag increased with increasing tip-speed ratio, as is to be expected.

At one distance (X/D = 1.67) the mean velocity, static pressure and turbulence profiles were measured for λ = 6.6.

From these measurements the terms in the axial momentum equation were evaluated in the following dimensionless form:

$$C_{T} = -4 \int \frac{U}{U_{\infty}} \left(\frac{\dot{U}}{U_{\infty}} - I \right) r' dr' : \text{total momentum flux} \qquad (eq. 1)$$

$$-2 \int \frac{\Delta P}{\frac{1}{2}\rho U_{\infty}^{2}} r' dr' : \text{effect of pressure difference}$$

$$-4 \int \frac{\Delta u'^{2}}{U_{\infty}^{2}} r' dr' : \text{turbulent momentum flux}$$

Fig. 6 shows the first two terms (as a function of the radial coordinate r'). The contribution of the longitudinal turbulence was found to be very small. The integrated values of the various terms in equation 1 are

momentum flux : 0.58

pressure : 0.19

turbulence : -0.02 $C_T = 0.75$

This value is very close to the $C_T = 0.74$ as measured with the drag balance. At larger distances the pressure disturbances quickly diminish; at X/D = 6.1 the integrated momentum flux already equals the drag.

These results show that one must be careful in estimating turbine drag (or performance) by looking at the velocity defect in the near-wake region.

turbulence

Measurements of longitudinal turbulence have been presented in ref. 2.

A plot of cross-wind profiles at different distances is reproduced in Fig. 7.

It shows that at X/D = 0.6 a marked peak is found at $Y/R \approx 1$.

This peak can be associated with the regular passage of the blade-tip vortices. The existence of these vortices form a typical difference between the wake of a wind turbine and that of, for instance, a porous gauze.

It is therefore of some interest to determine how far downstream these vortices can be found.

The following simple method was used to trace the position of the tip vortex system.

The output of a hot-wire anemometer traversing the wake was visualised on an oscilloscope. Outside the tip-vortex region a "normal" stochastic signal appeared, but when the probe moved into the vortex a very spiky signal emerged.

The cross-wind distance over which such a signal was found is plotted in Fig. 8 against the downstream distance.

It shows that the region over which the anemometer signal is "spiky" gradually broadens downstream.

At X/D = 2.1 determination of the beginning and the end of this region was not possible anymore, although the signal was still of a "spiky" nature.

A study of the frequency content of the velocity signal showed that the tip vortices could be found up to $X/D \approx 4$. The energy content associated with these frequencies is, however, very small, as depicted in Fig. 9.

It can therefore be concluded that from X/D $_{\approx}$ 4 the tip vortex system has completely disappeared.

3.2 Vertical axis wind turbine

program

In their study the wake of a full-scale (5.3 m) Darrieus turbine Vermeulen et al. (ref. 3) found large differences between full-scale and model results. These differences were attributed to the effect of atmospheric turbulence and to the different tip-speed ratios.

In order to eliminate the latter reason, additional wind tunnel measurements were carried out at various tip-speed ratios.

Contrary to the study of ref. 1, these additional measurements were performed in the uniform, low-turbulence flow case 3.

Unfortunately, the design of the support structure of the model is such that no force measurements can be executed. Moreover it is not possible to measure the aerodynamic power delivered by the turbine because of the large friction in the bearings of the model and of the DC-motor.

These friction losses are roughly 10 times larger than the estimated power production of the turbine.

So neither $C_T^{-\lambda}$ nor $C_p^{-\lambda}$ characteristics are known for this model, which reduces the usefulness of the present experiments somewhat.

It should also be pointed out that an essential difference between a horizontal-and a vertical-axis turbine is that the wake of the former is truly axial-symmetric, while the latter has a three-dimensional wake. This is illustrated by Fig. 10, which is a result of the multiple streamline calculation method of Strickland (see ref. 4). Simple integrations as carried out for instance using eq. 1 cannot be performed for the vertical-axis windlturbine, as long as the wake is not truly axial-symmetric.

For the present study only horizontal traverses were carried out.

wake measurements

Horizontal cross-wind profiles at X/D = 5 are plotted in Fig. 1! for different tip-speed ratios.

At all values of λ , the shape of the velocity defect profile is found to be asymmetric. Also, the position of the maximum defect is displaced from the centerline; for low λ it is at the positive Y, while it moves at higher λ 's towards the negative Y-direction.

The problem of asymmetry was earlier discussed by Vermeulen et al. (ref. 3), who found a very large displacement of the wake centerline (ca. 15 degrees). A review of the available literature suggested that "there are no Aerodynamic explanations for the wake centerline to be displaced by as much as 15 degrees". The deviations were therefore attributed to misalignments of the vane anemometers.

The present results of Fig. 1! show that the deviation is indeed rather small. The angle ϕ between the wake centerline and the mean flow velocity varies between +2 and -3 degrees, depending on the tip-speed ratio.

Also the deviations from symmetry are relatively small. It is therefore very reasonable that these deviations completely disappear when the approach flow is highly turbulent. The wind-direction fluctuations for the turbine test site of ref. 3 were in the order of 8 degrees (standard deviation), so it is unlikely that displacement effects of ca. 3 degrees can be found in the full-scale situation.

Fig. 12 shows the development of the wake at a tip-speed ratio of λ = 4.4. At first the shape is very asymmetric. With increasing distance the position of the maximum defect moves to the (-) y-direction till it reaches a steady position at X/D > 5. Also the shape of the velocity-defect profile becomes more symmetric at larger distances. This is illustrated by Fig. 13, where the measured cross-wind profile at X/D = 15 is plotted in universal coordinates. The cross-wind distance y' is measured from the assumed wake centerline.

It shows that only at the wake centerline some asymmetry remains; the edge of the wake is perfectly symmetrical.

The dotted curve is the gaussian error function:

$$\frac{U_{\infty} - U}{U_{0}} = \exp\left\{-0.693 \left(\frac{Y}{b}\right)^{2}\right\} \tag{2}$$

which is found to overestimate the velocity defect near the edges.

A summary of the measured wake development is given in Table 4.

A distinction is made between the real maximum defect and the defect that is found at the wind tunnel centerline (Y = 0), as is done in ref. 1.

The wake half-width is determined across the whole wake and divided by 2. Experience with other three-dimensional wakes has shown that these wakes approach axial-symmetry far down-stream. If it is assumed that at X/D = 15 the departures from axial-symmetry are small, it becomes possible to estimate the kinetic energy recovery in the wake.

In ref. 2 use is made of the parameter P/P_m :

$$P/P_{\infty} = \int_{0}^{1} 2 \left(\frac{U}{U} \right)^{3} r' dr'$$
(3)

which is a measure of the power available for a second wind turbine placed on the wake centerline (Table 4).

turbine drag coefficient

Again assuming the wake to be axial-symmetric at X/D = 15 it is possible to integrate the momentum loss for an estimate of the turbine drag coefficient $C_{\rm T}$ (using eq. 1).

It is found that $C_T = 0.50$ à 0.54 for $\lambda = 4.4$.

Experimental data on drag coefficients for Darrieus turbines are scarce. Muraca and Guillote (ref. 5) found $C_{\rm T}$ = 0.49 à 0.55 for a two-bladed turbine at λ = 4.4, which supports the value found by integrating the momentum loss.

comparison with previous results

The wake results of ref. 1 were obtained at λ = 5.5 for flow cases 1 and 2. Surveys were made at the wind tunnel centerline in the downstream direction, and cross-wind profiles were only measured at X/D > 10 from Y = -20 till Y = +20 cm.

Tabulated results can be found in Table 5.

Mind that these are <u>windtunnel</u> centerline values; Fig. 11 shows that these differ from the maximum defects.

It should also be remarked that the accuracy of the b/R values is rather poor.

In Fig. 14 a comparison is made between the present results and those obtained in flow case 1. At $\rm X/D < 5$ the present results are lower because the tip-speed ratio and therefore the drag is lower. As the turbulence intensity is only 1% insteam of 3.5% the rate of decay is also smaller for the Case 3 results.

At large distances the decay rate approaches the universal value of -2/3.

comparison with full-scale data

Fig. 15 presents a comparison between the present Case 3 results and the data obtained in ref. 3.

This figure reflects the importance of the ambient turbulence as for Case 3 the turbulence intensity is 1%, while for the full-scale situation the turbulence intensity was estimated to be 20%.

The largest differences are found in the region very close downstream of the turbine as the rate of decay further downstream is only slightly different.

The $U_{\rm O}/U_{\infty}$ versus X/D curve is seen to move to the left (small X/D) when the turbulence intensity is increased. This is also the case for the horizontal-axis wind turbine (Fig. 4). This effect of turbulence on the length of the so-called near wake region is further discussed in par. 4.

Their seems also to be a difference in the value of $U_{_{\rm Q}}/U_{_{\infty}}$ for small X/D. It is of interest to compare cross-wind profiles at downstream distances which are more or less characteristic for the end of the near-wake region.

Fig. 16 compares the wind tunnel results at X/D = 3 with full-scale data of ref. 3 (Fig. 9 of ref. 3, with the Y = 0 axis chosen as $\Delta\beta = -12.5^{\circ}$).

Fig. 16 shows that the profile at low turbulence intensity is more "peaked" than at high intensity; i.e. the full-scale profile is more flattened.

This is the reason why the values of $\mathrm{U}_{\mathrm{O}}/\mathrm{U}_{\mathrm{\infty}}$ are different.

This difference is, however, of minor importance because the differences in momentum flux associated with it are only small.

It can therefore be concluded that the only difference of importance between the windtunnel wake and the full-scale wake is the length of the near-wake region.

comparison with the horizontal-axis turbine

When one wants to compare the wake of a vertical- and a horizontal-axis wind turbine, the problem arises of how to choose an equivalent tip-speed ratio λ . In general, there are three possibilities

- 1) similar λ
- 2) λ corresponding to similar drag $\mathbf{C}_{\mathbf{T}}$
- 3) λ corresponding to the optimum power C_{p} .

The ultimate choice clearly depends on the object of the comparison. In Fig. 17 the second possibility is chosen by comparing the present results for λ = 4.4 with the horizontal-axis data for λ = 5 (there is a slight difference in drag coefficient, however).

Plotted are centerline velocity differences and wake half-widths against downstream distance showing a very similar behaviour.

It must be remarked, however, that for X/D < 15 the shape of the cross-wind profiles is very different, as was discussed earlier.

At larger distances both b/R and $\rm U_{o}/\rm U_{\infty}$ compare very well between both types. It can be concluded therefore that not only the wake development in the far wake is independent of the type of windturbine but that also the exact values of the wake parameters b/R and $\rm U_{o}/\rm U_{\infty}$ are very identical, provided the turbine drag coefficient is the same.

4. EMPIRICAL WAKE MODEL

In ref. 6 a study is reported on the development of axial-symmetric wakes behind porous gauzes imbedded in turbulent boundary layers.

The resulting data were used to construct a simple wake model for the calculation of the development of wind-turbine wakes.

In the model two downstream regions are distinguished:

A) Near-wake region

This is the region close behind the turbine, which is in fact of minor importance for the analysis of wake interaction effects in wind-turbine clusters. So a very simple model description has been chosen.

It has also been chosen because it is similar to the one as used by Lissaman and Bate (ref. 7) for their analysis of the wake of a wind turbine. This definition proved to be very useful for the description of the wake development. It is based on several assumptions regarding the near-wake structure of a wind turbine.

Fig. 18 (after ref. 7) shows the assumed geometry of the wake behind the wind turbine.

A short distance downstream from the turbine, the uniform entering velocity profile \mathbf{U}_{∞} is assumed to have changed to an other uniform velocity profile \mathbf{U}_{2} . The region where this velocity \mathbf{U}_{2} remains constant, is called the potential core.

The velocity reduction $U_{\infty} - U_2$ is determined by the working conditions of the wind turbine, or, which is the same, by the drag of the turbine. Note that U_2 is not the velocity through the rotor plane, but the velocity at the inviscid expanded rotor disk (see ref. 7).

The axial momentum theory for a power extraction dis is then used to calculate the relationship between the drag and the velocity reduction $\rm U_{\infty}$ - $\rm U_2$:

$$T = \frac{1}{2} \rho + \Pi D^{2} \left(U_{\infty}^{2} - U_{2}^{2}\right)$$
 (4)

With the definition of the drag coefficient:

$$C_{T} = \frac{T}{\frac{1}{2} \rho \frac{1}{4} \prod D^{2} U_{\infty}^{2}}$$

it follows that the initial velocity difference $\left(\frac{U_o}{U_\infty}\right)_{X=0}$ is related to the turbine drag by:

$$\begin{pmatrix} \frac{U_o}{U_\infty} \end{pmatrix}_{X = 0} = 1 - \frac{U_2}{U_\infty} = 1 - \sqrt{1 - C_T} \tag{5}$$

As the flow proceeds downstream, the exterior flow mixes with the edge of the potential core and after the distance $X_{N.W.}$ the potential core is completely eroded.

This erosion of the potential core is the result of turbulent mixing by:

- 1°) the ambient turbulence
- 20) the generated turbulence
 - the turbulence generated by the velocity gradients at the edge of the potential core, i.e. of U_{∞} U_{2} . This is a function of the turbine drag (eq. 4) and thus of λ ;
 - the turbulence generated by the wind turbine itself, like bladetip- and hub vortices. This depends on the type of wind turbine, the blade loading and the tip-speed ratio.

The functional relationship between the near-wake length $X_{N.W.}$ and the above-mentioned eroding factors should be experimentally determined.

The near-wake length can be evaluated as that value of X/D where the line for $\frac{U_O}{U_\infty} = 1 - \sqrt{1 - C_T}$ crosses the measured $\frac{U_O}{U_\infty}$ versus X/D curve. This was already done in ref. 6.

The results of ref. 6 and ref. 3, together with the present results are gathered in Fig. 19.

It can be concluded that

- a) increasing turbulence results in a decrease of the near-wake length;
- b) increasing turbine drag also reduces the near-wake length;
- c) their seems to be little effect of the type of wind turbine.

B) Far-wake region

In the region following the near-wake region, the centerline velocity difference decays as

$$\frac{U_o}{U_\infty} \approx \left(\frac{X}{D}\right)^d \tag{6}$$

In ref. 6 it was found that for turbulent flows of turbulence intensity larger than 6%, the decay rate d equals d = -1.25.

But also when the ambient turbulence is below 6% a region can be found where the decay rate d = -1.25.

This is plausible because the turbulence generated by the object itself is also quite high. This suggests that the addition of "extra turbulence" (induced by the object + ambient turbulence) does not affect the rate of decay any more when the level of this extra turbulence is above a certain critical value. When the "extra turbulence" level is higher than this critical value, the rate of decay is ca. -1.25, and when the level is below this critical value the rate of decay becomes smaller.

It decreases with decreasing "extra turbulence" until the self-preserving state is reached. Both experimentally and theoretically it has been found that the decay rate of the centerline defect for a uniform, low-turbulence flow is -2/3.

For most practical cases - i.e. wind turbines in atmospheric shear flow - the decay rate of an axial-symmetric wind turbine wake will therefore be d = -1.25. The data of ref. 6 also show that within the far-wake region, the velocity defect profile can be approximated by the Gaussian error curve (eq. 2). When this is the case, the momentum flux can be easily integrated, which results in the following equation for the wake half-width in the far-wake region:

$$C_{T} = -2.89 \left(\frac{b}{R}\right)^{2} \left[\frac{U_{o}}{U_{\infty}}\right]^{2} - \frac{U_{o}}{U_{\infty}}$$
 (7)

The following set of equations can now be used as a simple way of calculating the wake of a wind turbine (without ground effects!, see ref. 6).

- a) determine near-wake length $X_{N,W}$ using Fig. 19
- b) far-wake region: X > X_{N.W}

$$\frac{\text{velocity profile}}{1 - \frac{U}{U_{\infty}} = \frac{U_{0}}{U_{\infty}} \exp \left\{ -0.693 \left(\frac{y}{b} \right)^{2} \right\}$$

centerline defect

$$\frac{U_{o}}{U_{\infty}} = (1 - \sqrt{1 - C_{T}}) \cdot \left(\frac{X}{X_{N.W}}\right)^{-1.25}$$

wake half-width

$$\frac{b}{R} = \left[\frac{-c_T}{2.89 \left[\frac{1}{2} \left(\frac{U_o}{U_\infty} \right)^2 - \frac{U_o}{U_\infty} \right]} \right]^{\frac{1}{2}}$$

c) near-wake region: $X < X_{N.W}$

For most practical cases not of interest since X $_{N.W}$ \approx $2\frac{1}{2}$ D. Therefore only centerline defect is calculated as:

$$\frac{U_{o}}{U_{\infty}} = 1 - \sqrt{1 - C_{T}}$$

5. CONCLUSIONS

Additional measurements have been performed on the wake structure of both horizontal-axis and vertical-axis wind turbines.

The following conclusions can be drawn:

For the horizonral-axis wind turbine

- The contribution of the pressure term in the axial momentum equation is of non-neglible magnitude in the near-wake region.
 This is of importance when evualuating the performance of a wind turbine using wake measurements at small downstream distances.
- 2) The vortices trailing from the blade tips are found to disintegrate rather quickly; even in a uniform low-turbulence flow they disappear within several diameters distance downstream of the turbine.

For the vertical-axis wind turbine

- 3) Close to the turbine and in low-turbulence flows, the wake is found to be asymmetric. The amount of asymmetry is, however, small. It is therefore expected to disappear when the approach flow is more turbulent.
- 4) At larger distances from the turbine, the wake becomes more symmetric till it reaches a symmetric state at X/D \approx 15 à 20 (for low-turbulence flows).
- 5) A comparison with wake data obtained with a full-scale 5.3 m turbine shows that the intense turbulence in the atmosphere has a large influence on wake development, especially on the length of the so-called "near-wake" region

It can also be concluded that the wake development, in terms of centerline velocity defect and half width, is independent of the type of wind turbine provided that both have the same drag coefficient.

Based on the measurements, an empirical wake model is proposed to estimate the mean wake structure of a wind turbine.

REFERENCES

- [1] Boschloo, G.,
 Wake structure of a Darrieus rotor,
 TNO-Report 77-0724 (1977, in Dutch).
- [2] Vermeulen, P.,
 A wind-tunnel study of the wake of a horizontal axis wind turbine,
 TNO-Report 78-09674 (1978).
- [3] Vermeulen, P., Builtjes, P., Dekker, J., Lammerts v. Bueren, G.,
 An experimental study of the wake behind a full scale vertical-axis wind turbine
 TNO-Report 79-06118.
- [4] Strickland, I.H.,

 A performance prediction model for the Darrieus turbine,

 Proc. Int. Symp. Wind-Energy Syst. Cambridge, Sept. 7-9, 1976.
- [5] Muraca, R.I., Guillotte, R.I.,
 Wind tunnel investigations of a 14 ft. vertical axis windmill,
 NASA TM-X-72663 (1976).
- [6] Vermeulen, P.,
 Mixing of simulated wind turbine wakes in turbulent shear flow.
 TNO Report 79-09974 (1979).
- [7] Lissaman, P.B.S., Bate, E.R.

 Energy effectiveness of arrays of wind energy conversion systems (1977)

 Aero Vironment report AVFR 7058

WAKE RESULTS HORIZONTAL-AXIS WINDTURBINE

flow case	λ	X/D	U _o U _w	$\frac{b}{R}$
1	6.6	1.7	0.66	0.96
		3.3	0.56	0.86
		6.1	0.29	1.01
		9.2	0.19	1.17
2	6.6	1.7	0.66	0.92
		3.3	0.55	0.79
	=	6.1	0.29	1.00
U		9.2	0.18	1.17
3	5	1.7	0.53	0.97
		3.3	0.46	0.89
		6.1	0.38	0.82
		9.2	0.26	0.92
	6.6	1.7	0.65	1.00
		3.3	0.57	0.89
		6.1	0.40	0.89
		9.2	0.24	1.08
	8.5	1.7	0.73	1.06
		3.3	0.68	0.92
		6.1	0.39	1.00
		9.2	0.20	1.25

CENTERLINE VELOCITY DEFECT

Case 3 Horizontal-Axis Windturbine

Distance X/D	Velocity Defect $\frac{U}{U_{\infty}}$				
	λ = 5.0	λ = 6.6	$\lambda = 8.5$		
1.1	0.60	0.81	0.77		
1.7	0.53	0.65	0.73		
2.2	0.49	0.64	0.72		
2.8	0.46	0.61	0.69		
3.3	0.46	0.57	0.68		
3.5	0.46	-	0.67		
3.9	-	0.57	-		
4.2	0.43	-	0.59		
4.4	-	0.54	-		
4.9	- ,	-	0.49		
5.0	_	0.49	-		
5.6	0.39	0.45	0.40		
6.1	0.38	0.40	0.39		
6.9	0.32	-	0.30		
7.5		0.32	-		
8.3	0.28	0.28	0.21		
9.2	0.26	0.24	0.20		
10.0	-	0.22	-		
11.1	0.20	0.21	0.153		
12.5	0.179	0.175	0.130		
13.8	0.152	0.156	0.114		

CENTERLINE VELOCITY DEFECT Horizontal-Axis Windturbine tip-speed ratio λ = 6.6

Distance X/D	Velocity Defect $\frac{U_{o}}{U_{\infty}}$			
*	Case 1	Case 2		
1.1	0.73	0.71		
1.7	0.66	0.66		
2.2	0.61	0.60		
2.8	0.59	0.58		
3.3	0.56	0.55		
3.9	0.51	0.48		
4.4	0.43	0.42		
5.0	0.37	0.36		
5.6	0.32	0.33		
6.1	0.29	0.29		
7.5	0.23	0.22		
8.3	0.198	0.187		
9.2	0.187	0.174		
10	0.164	0.162		
11.1	0.142	0.142		
12.5	0.125	0.122		
13.8	0.107	0.105		

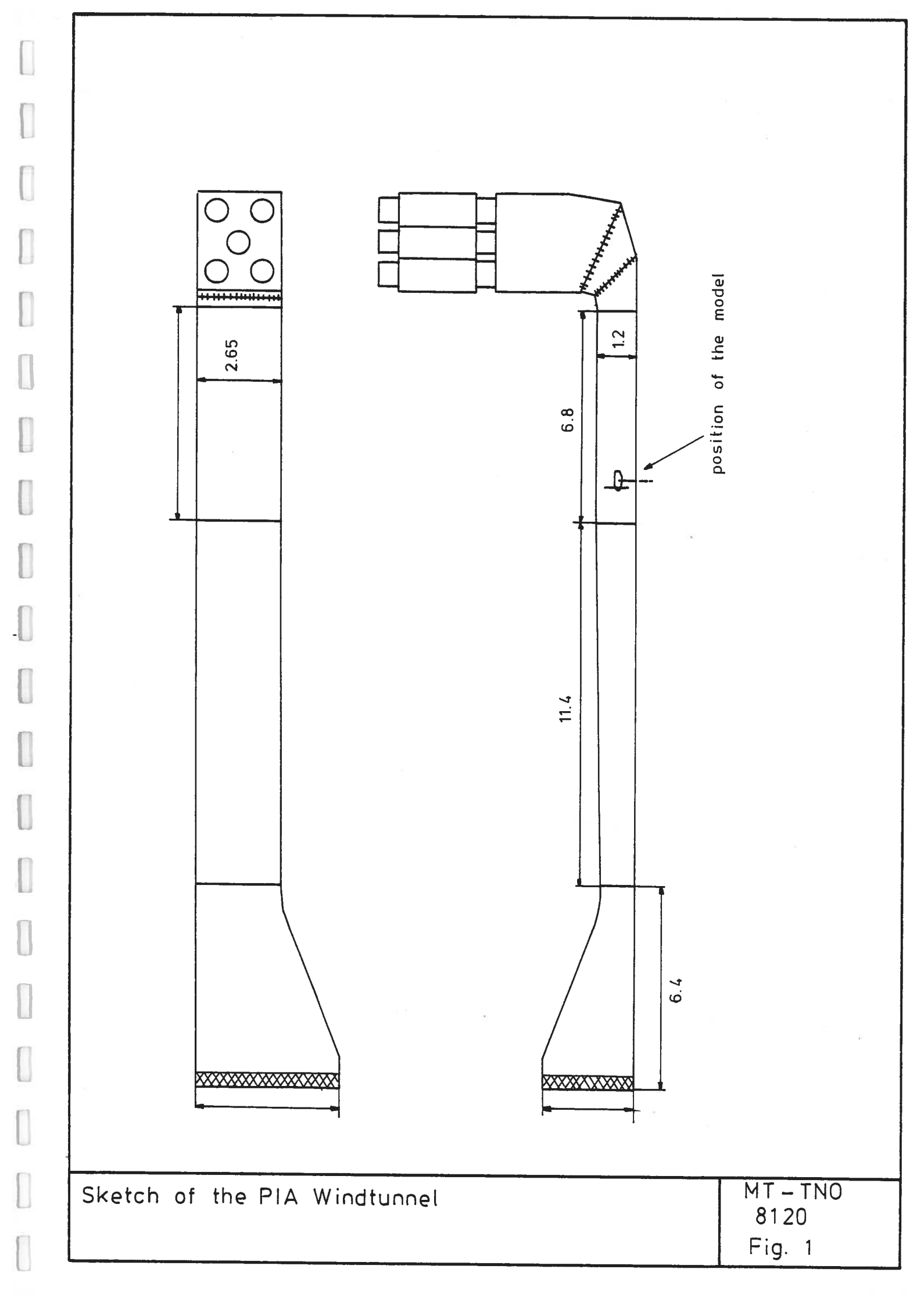
WAKE RESULTS VERTICAL-AXIS WIND TURBINE, CASE 3 Flow Case 3, tip-speed ratio λ = 4.4

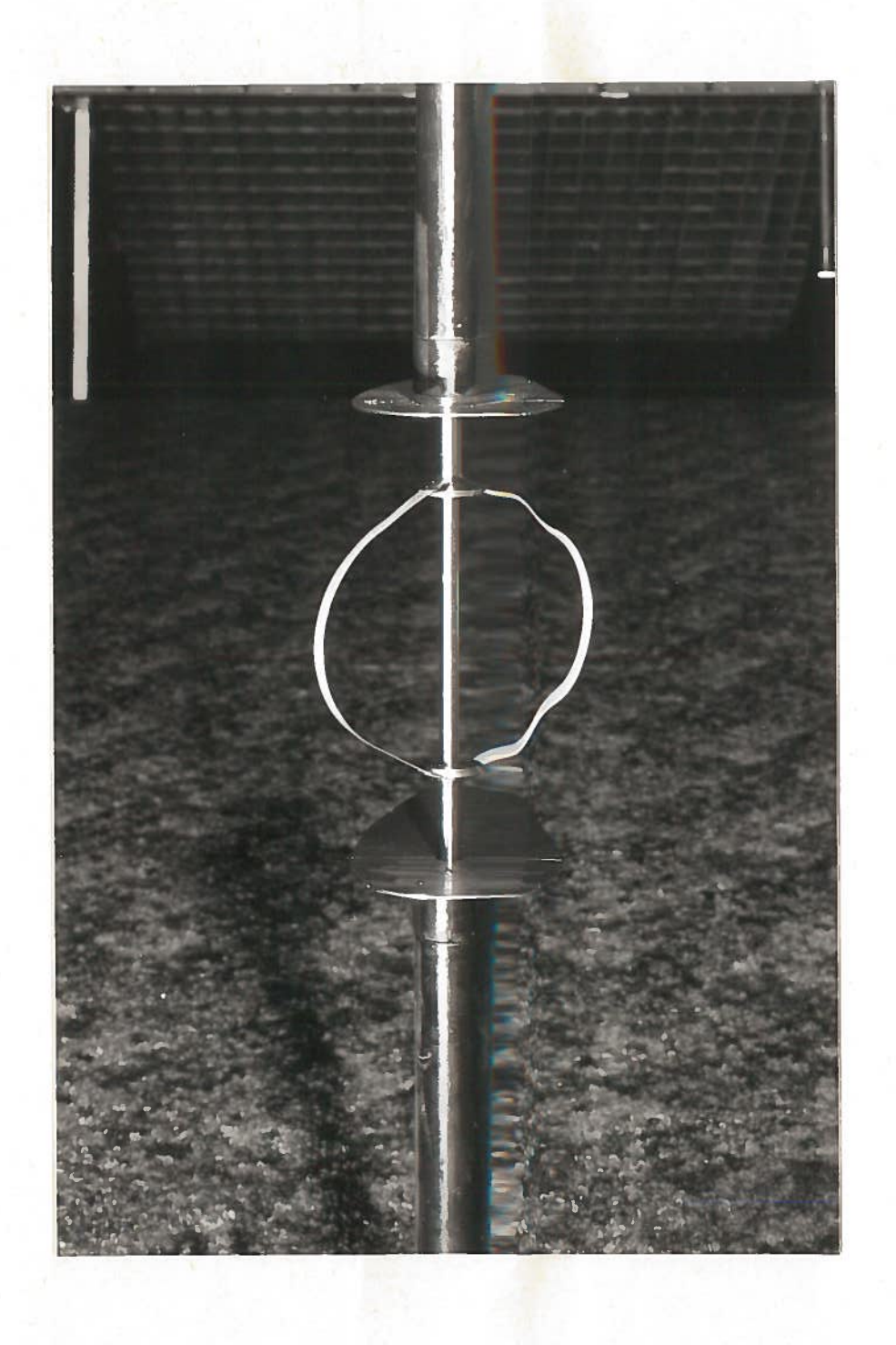
Distance X/D	Defect U _O /U _∞	t Մ _o /Մ _∞	Half width (horizontal)	Kinetic Energy		
Α, υ	Y = 0	Maximum	b/R	P/P _∞		
1.5	0.73	0.73	0.82*	-		
3	0.62	0.62	0.81*	-		
5	0.41	0.44	0.78*	-		
10	0.20	0.21	1.10	-		
15	0.135	0.142	1.33	0.68		
20	0.100	0.113	1.50	0.75		

^{*} profile very asymmetric

WAKE RESULTS VERTICAL-AXIS WIND TURBINE Case 1 and 2 (ref. 1) tip-speed ratio λ = 5.5

Distance	flow case 1			flow case 2			
X/D	U _o	b/R	P/P _∞	ប <u>ប</u>	<u>O</u>	P/P_{∞}	
1	0.81						
2	0.84						
2.5	_			0	.69		
3	0.76						
4	0.57						
5	0.42			0	.31		
6.25	0.32						
7.5	0.26			0	.19	0.62	22
8.75	0.20			:			
10	0.18	1.5	0.55	0	.15	0.69	
12.5	0.145	N.		2 2	İ		
15	0.124	1.7	0.70	0	.10	0.77	· ⁷
20	0.088			0	.084		





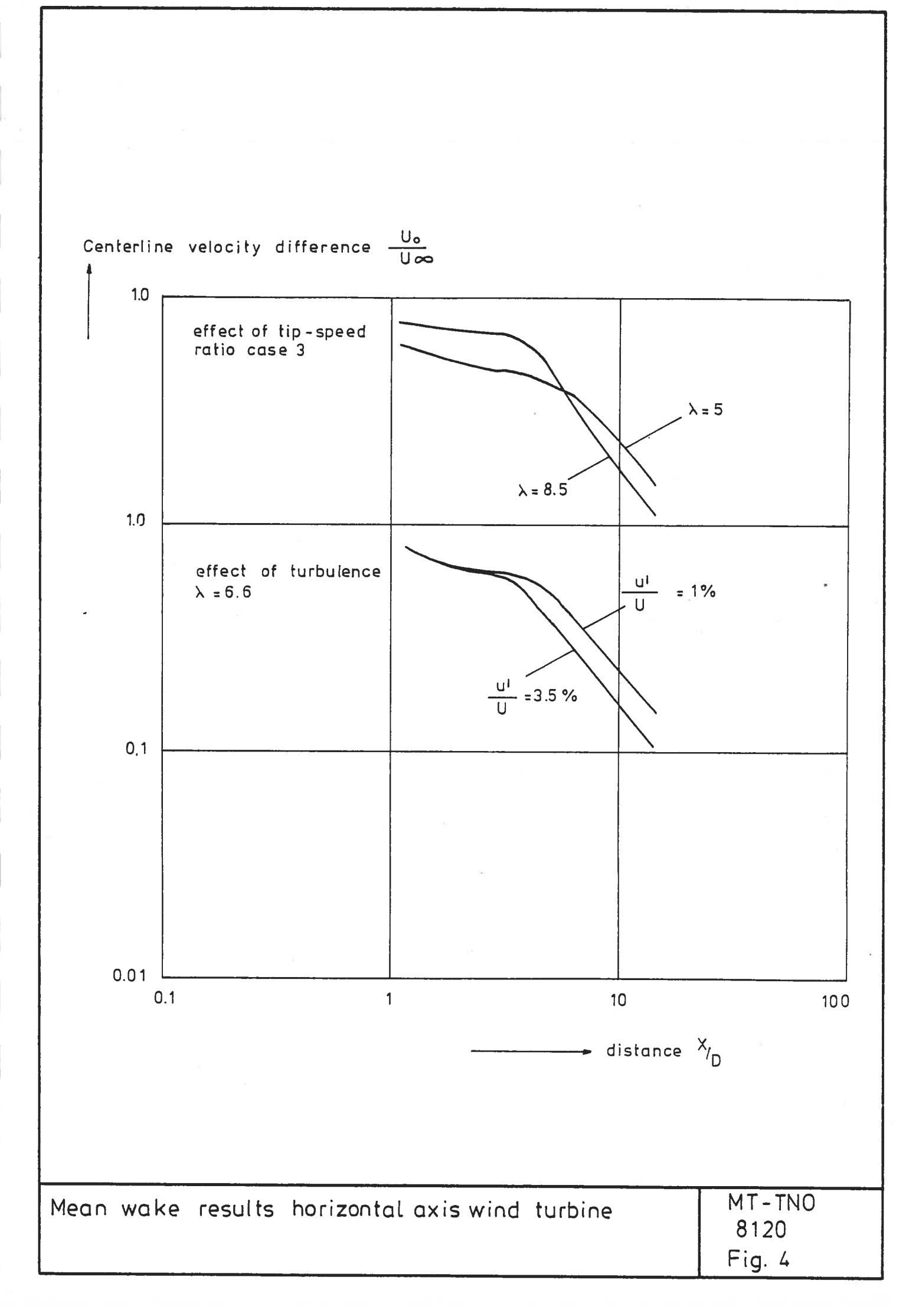
Vertical axis wind turbine

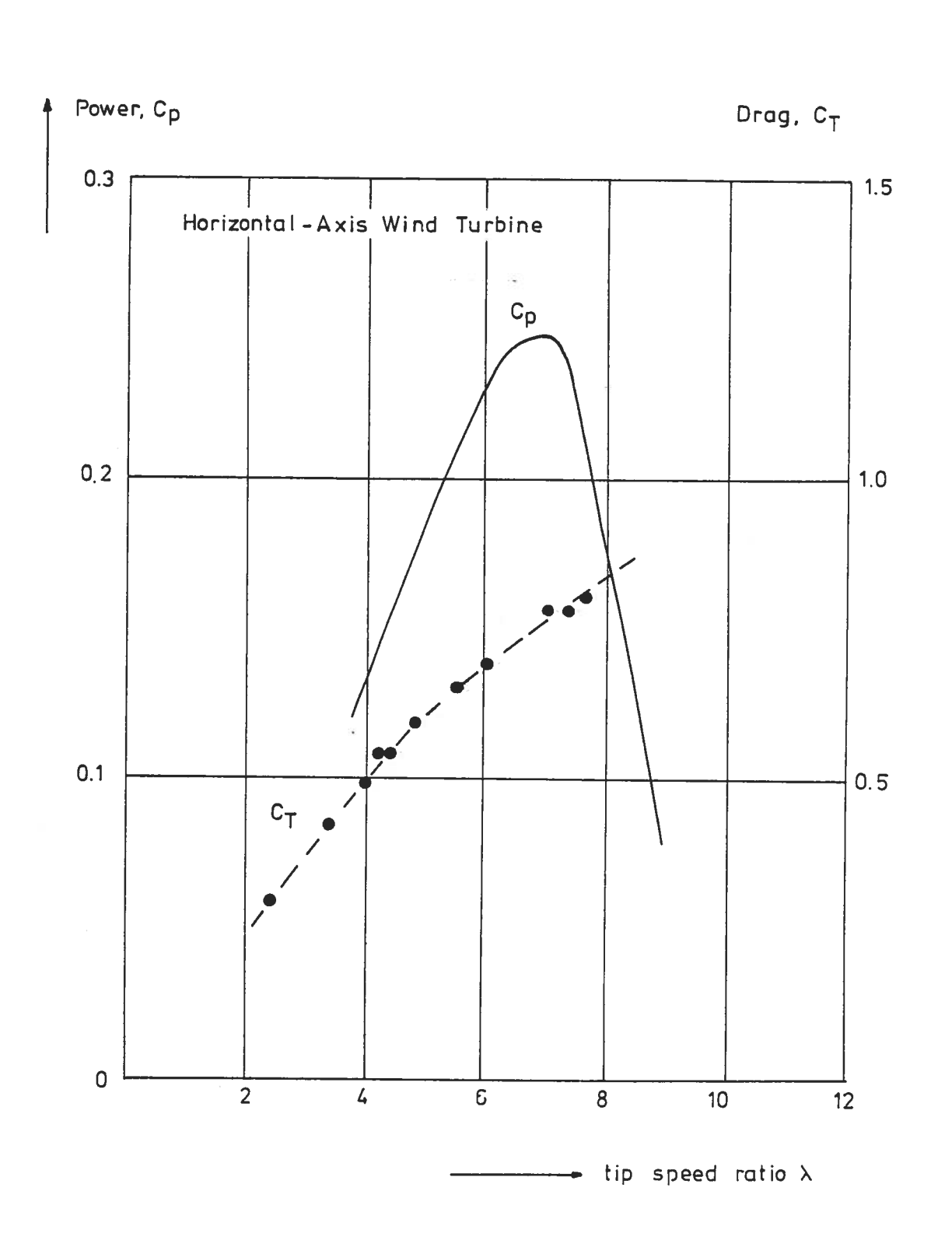
MT-TNO 8120 Fig. 2



Horizontal axis wind turbine.

MT-TNO 8120 Fig. 3



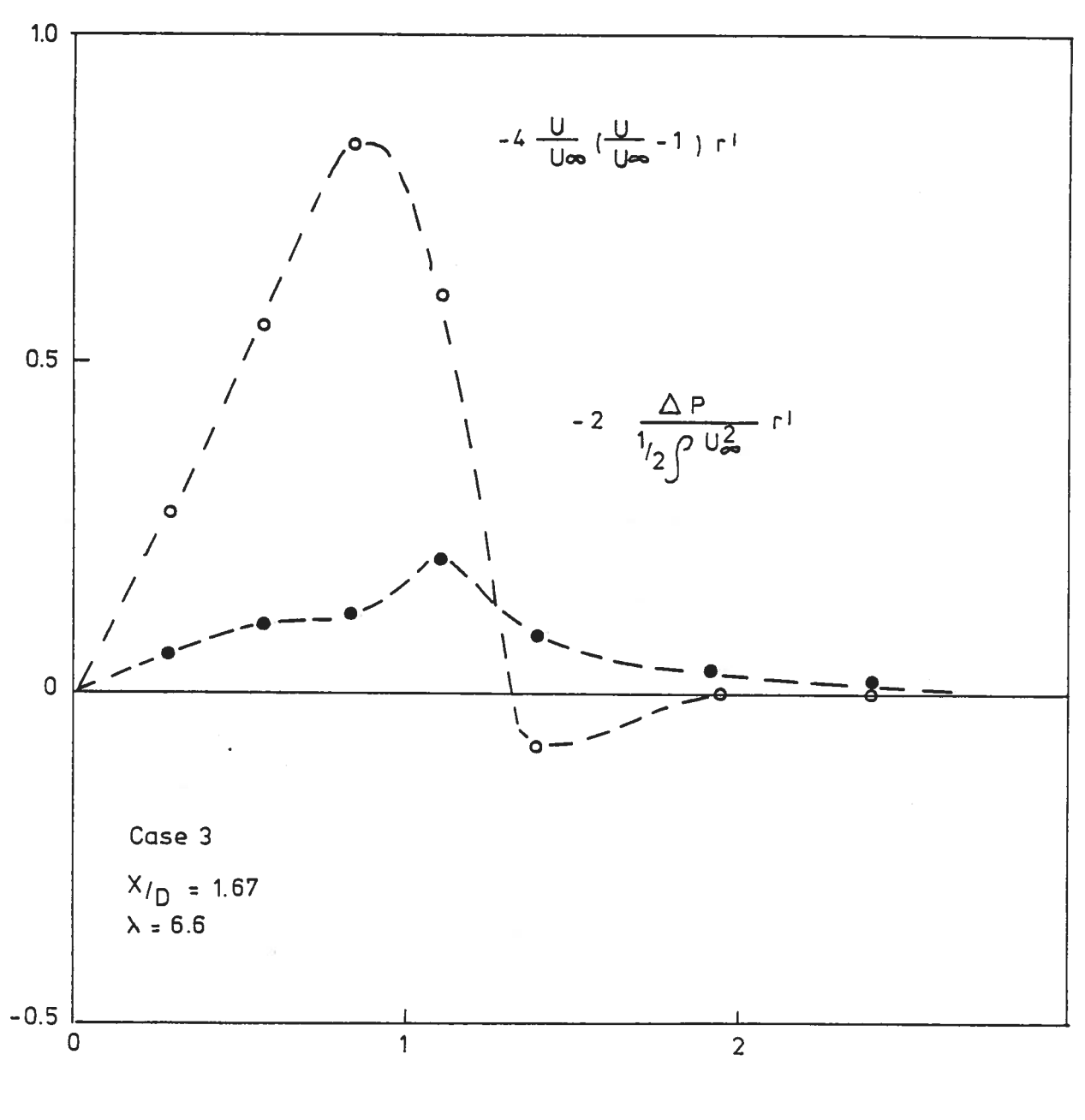


Power and Drag of the horizontal axis machine as a function of the tip-speed ratio

MT TNO 8120

Fig 5

terms in momentum balance

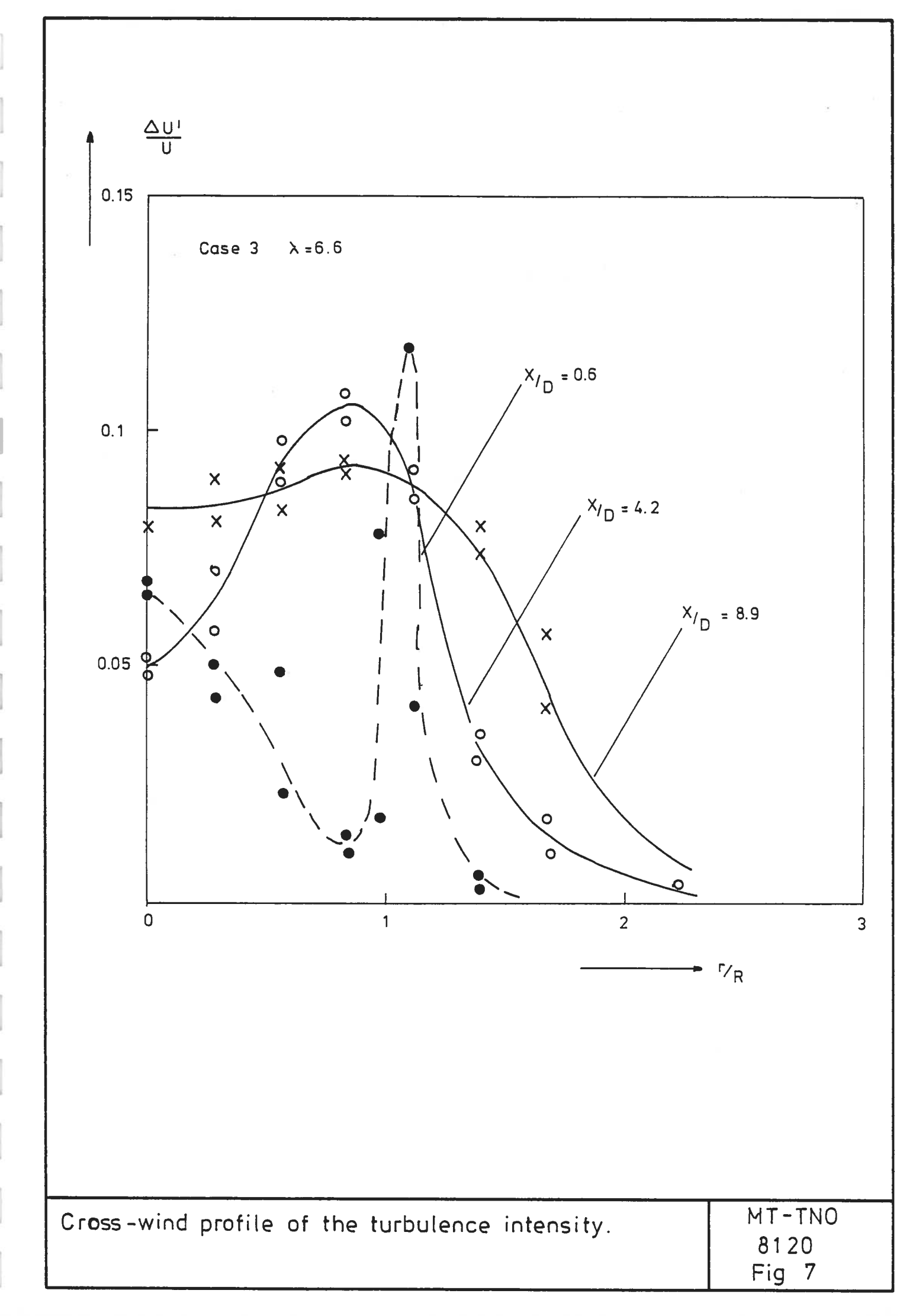


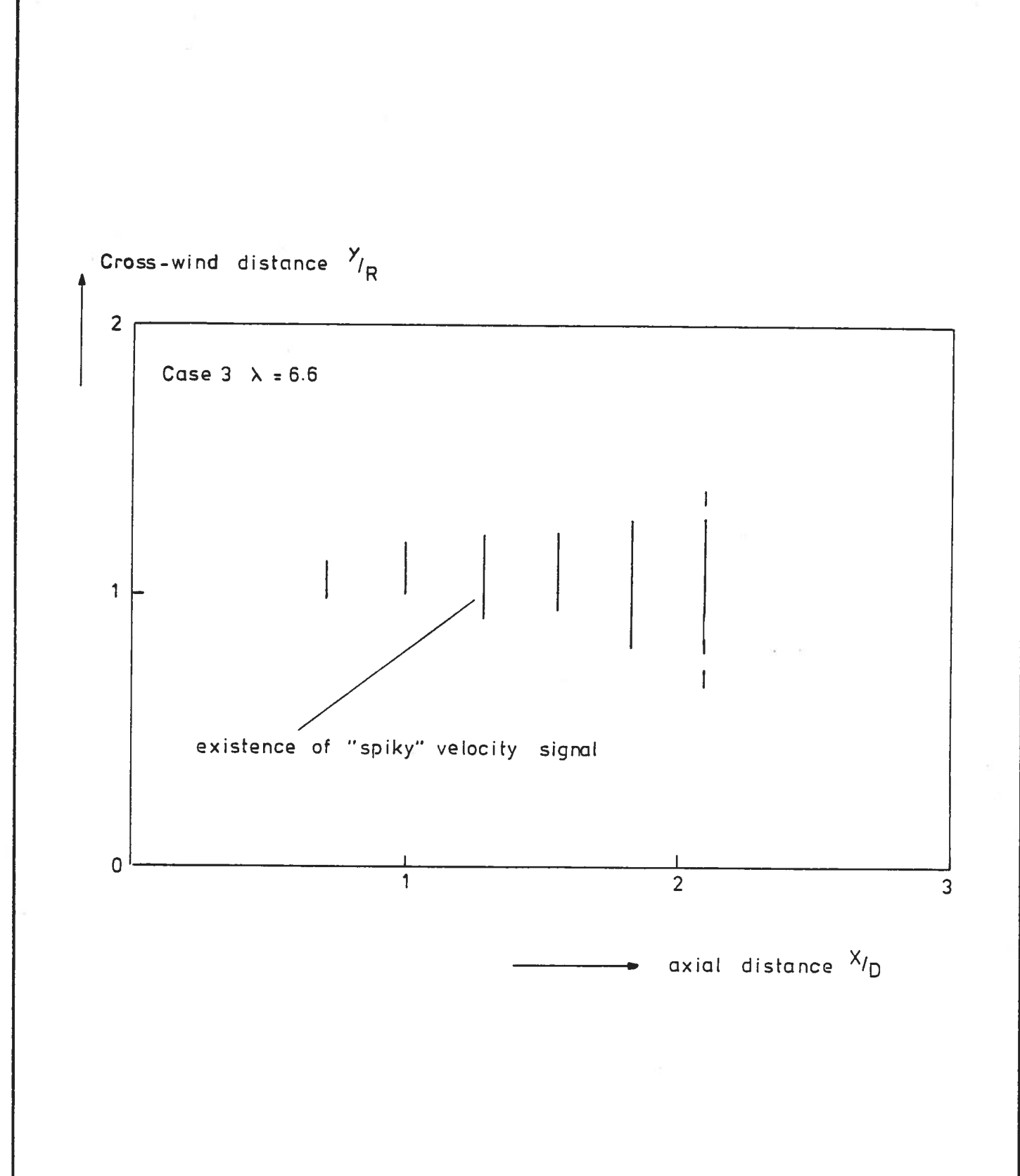
cross - wind distance r!

Contributions of momentum flux and pressure to the momentum balance

MT - TNO 8120

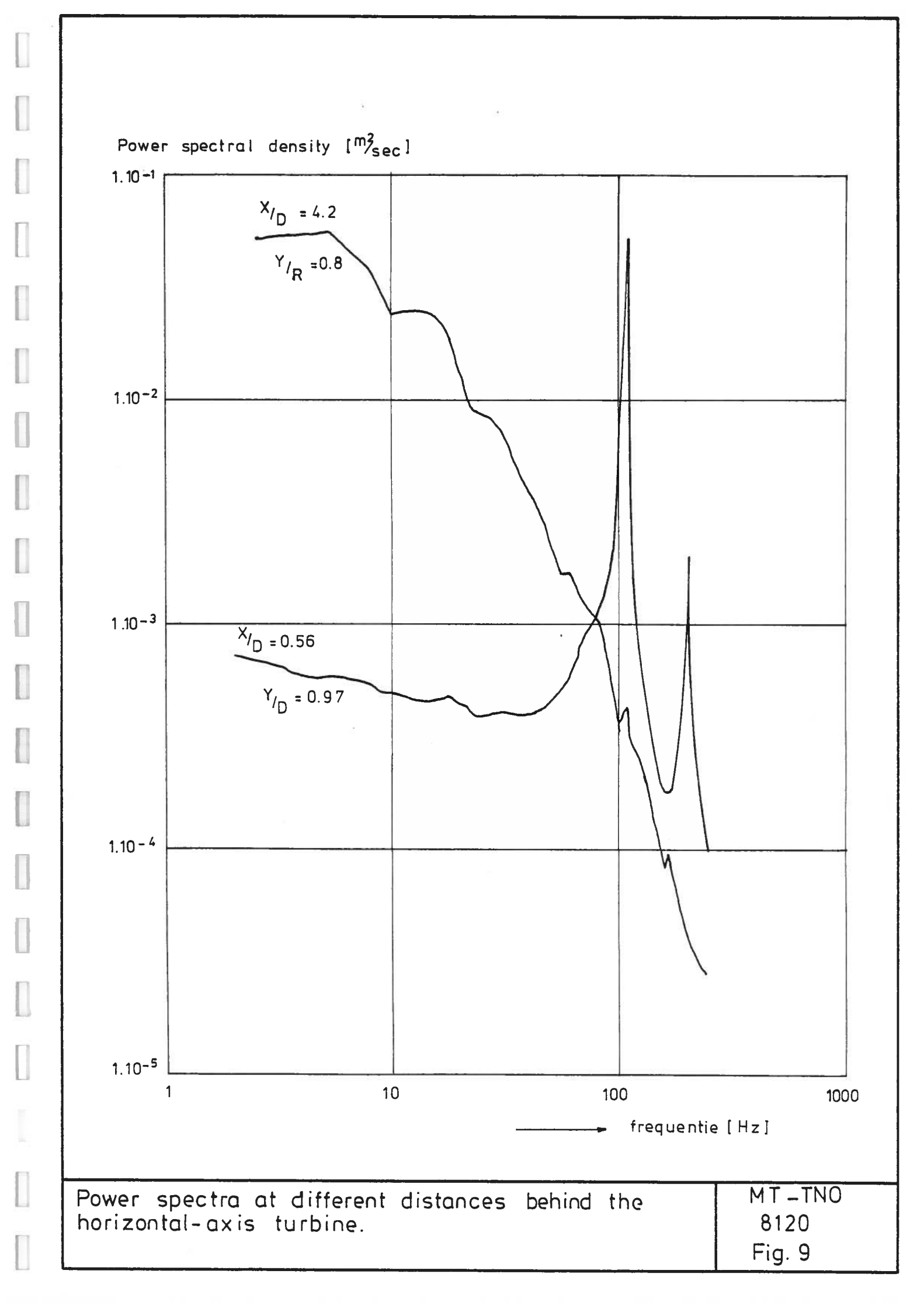
Fig. 6

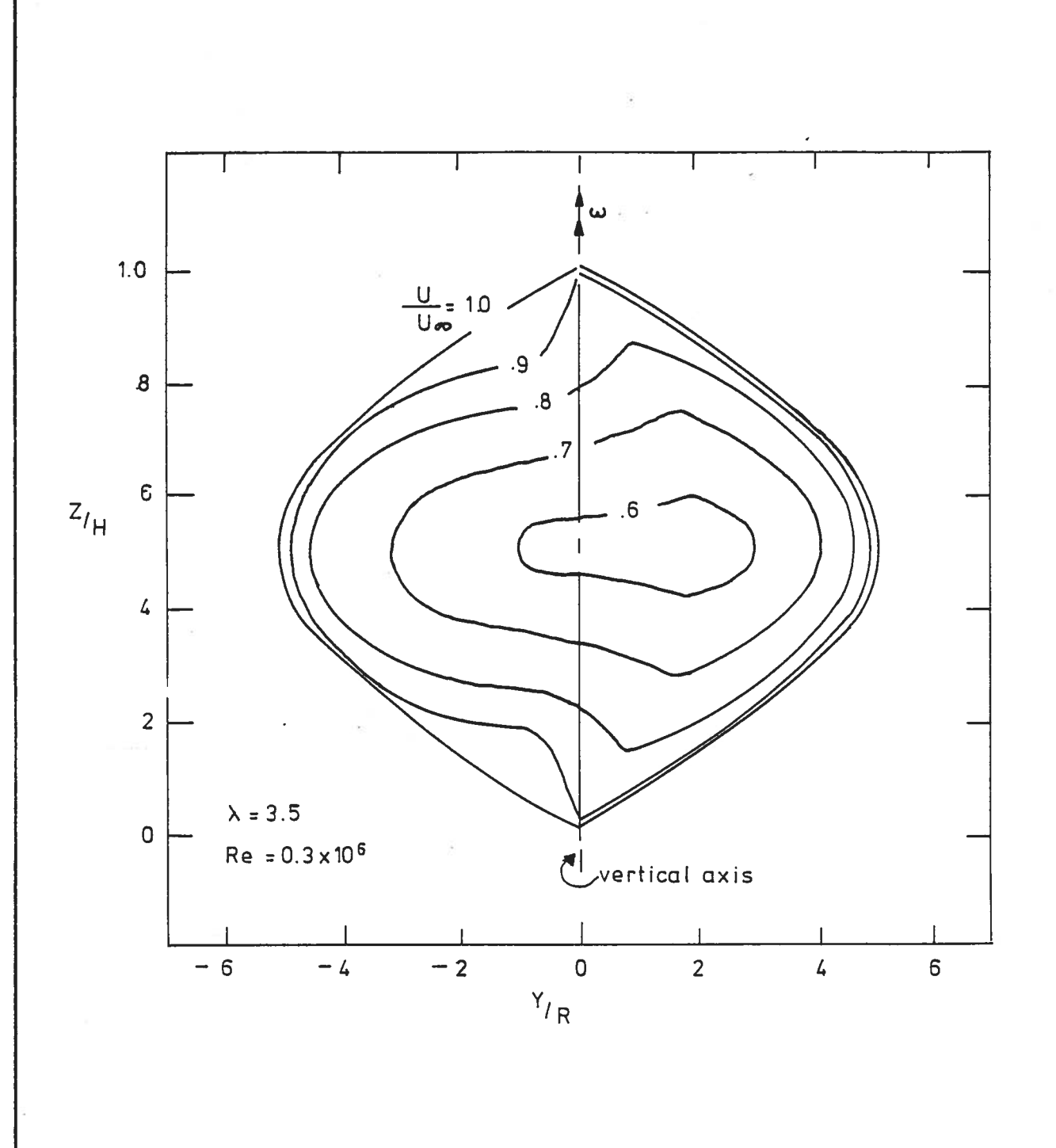




Position of tip vortex system behind the horizontal axis wind turbine.

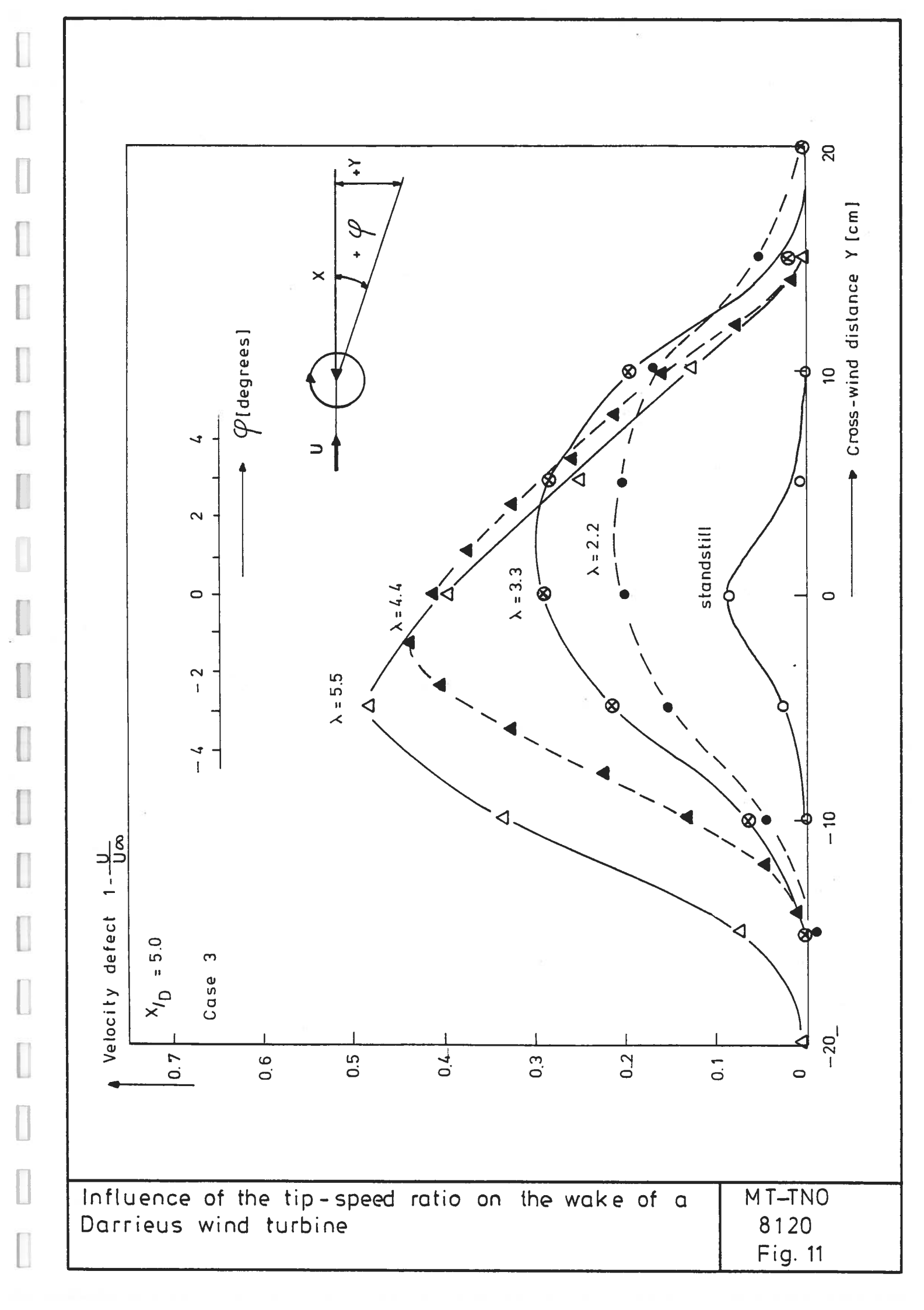
MT-TNO 8120 Fig. 8

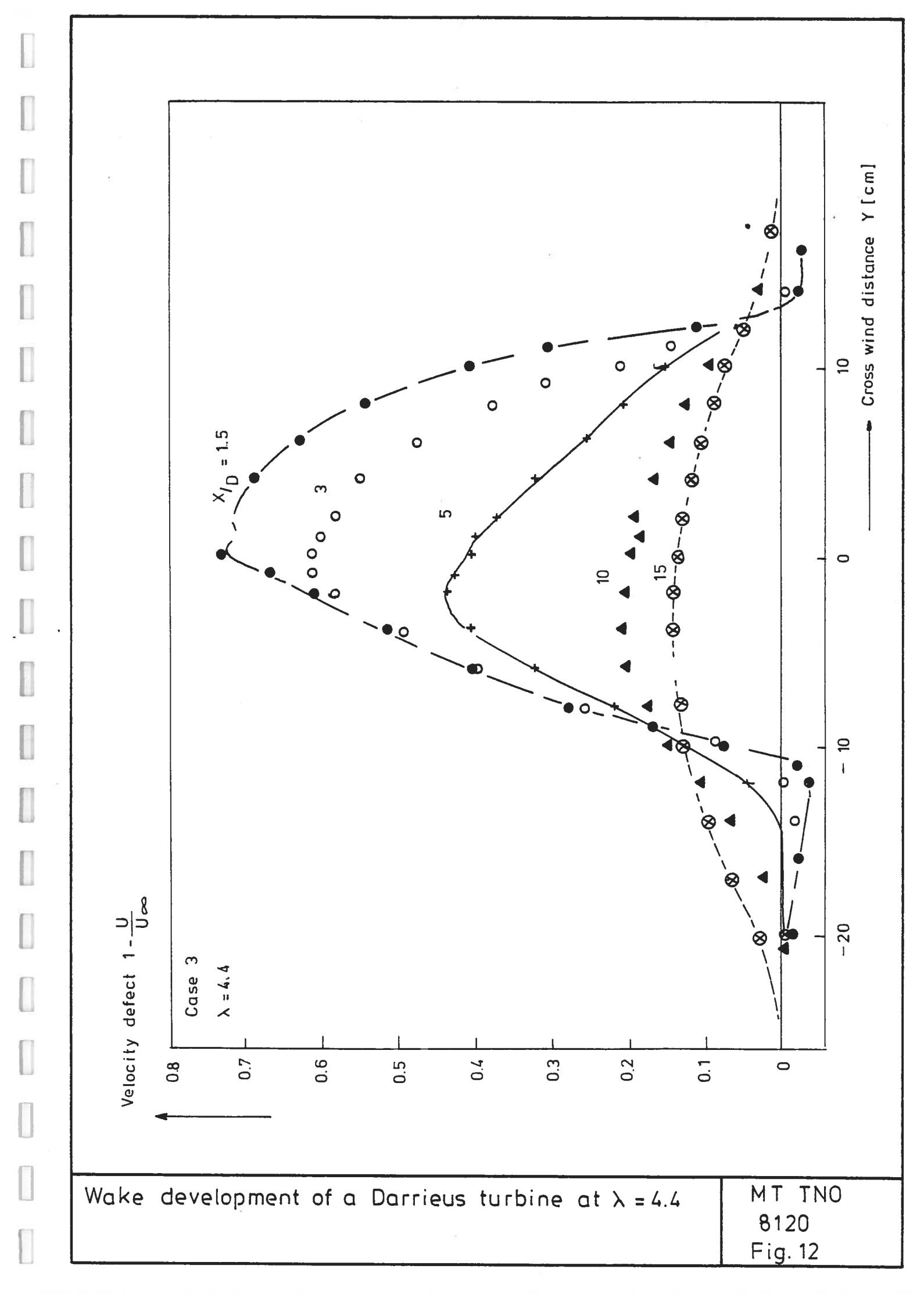


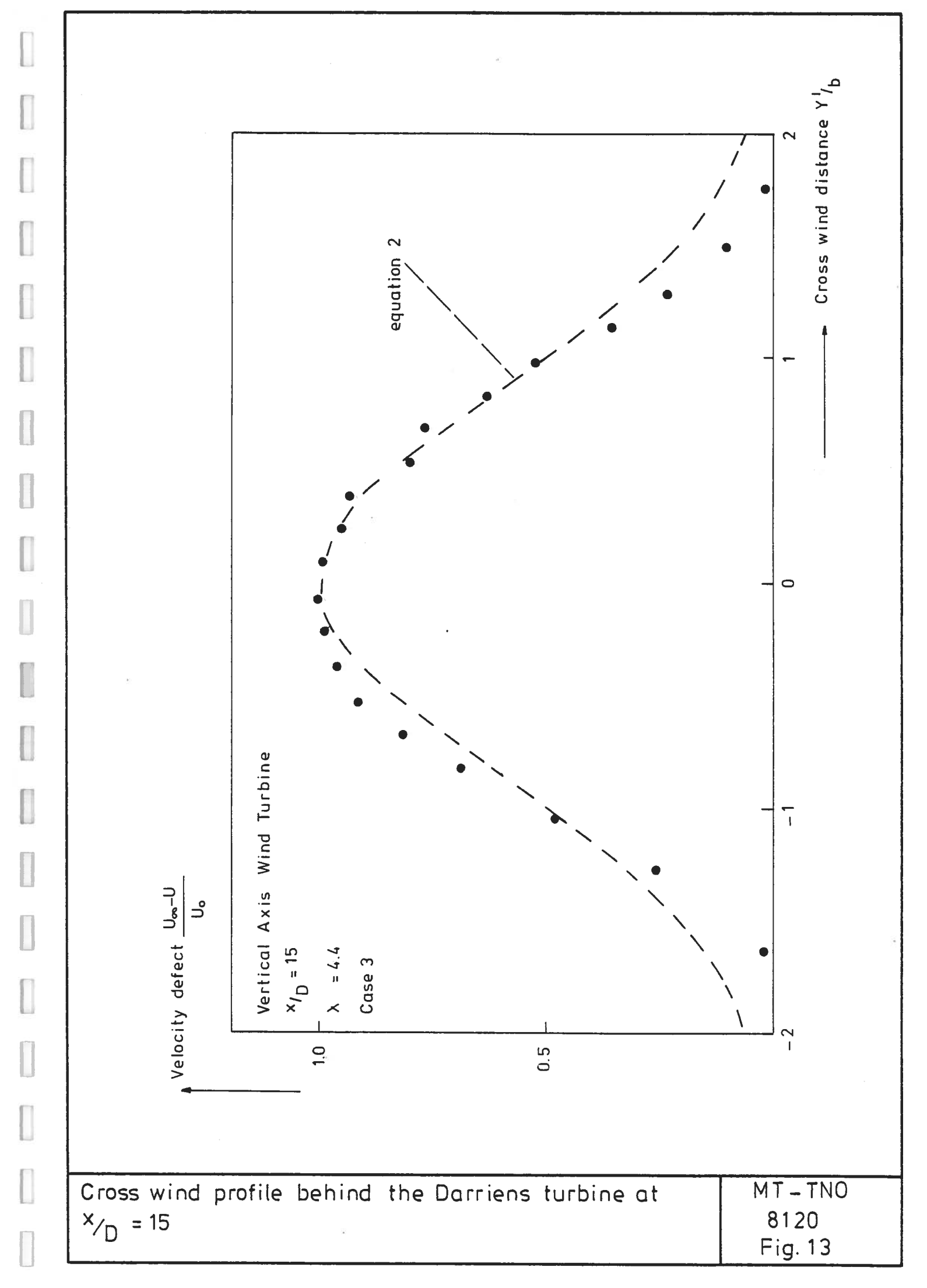


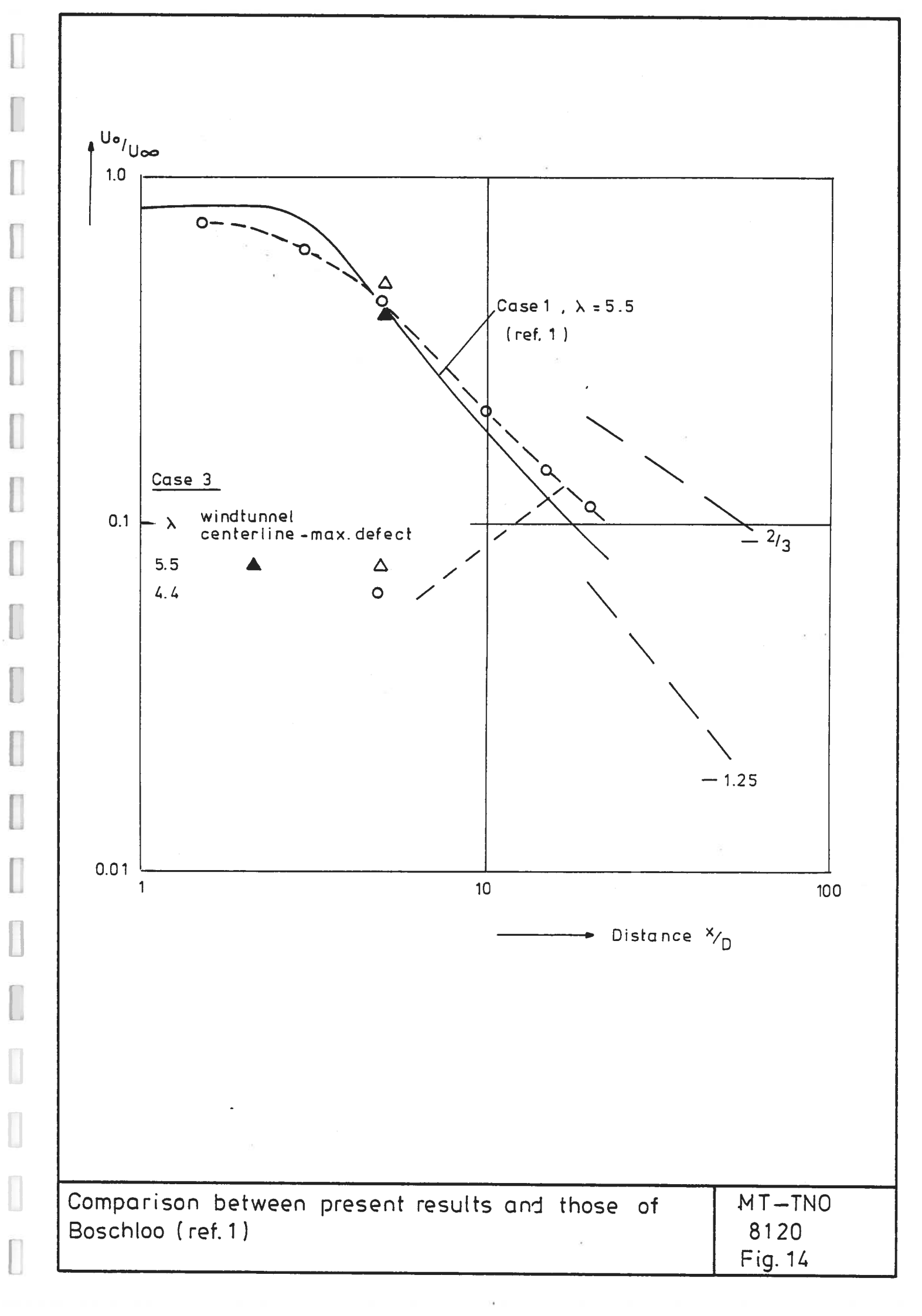
Variation of Streamtube Velocities Through the Rotor (View Looking Upstream Through the Rotor)

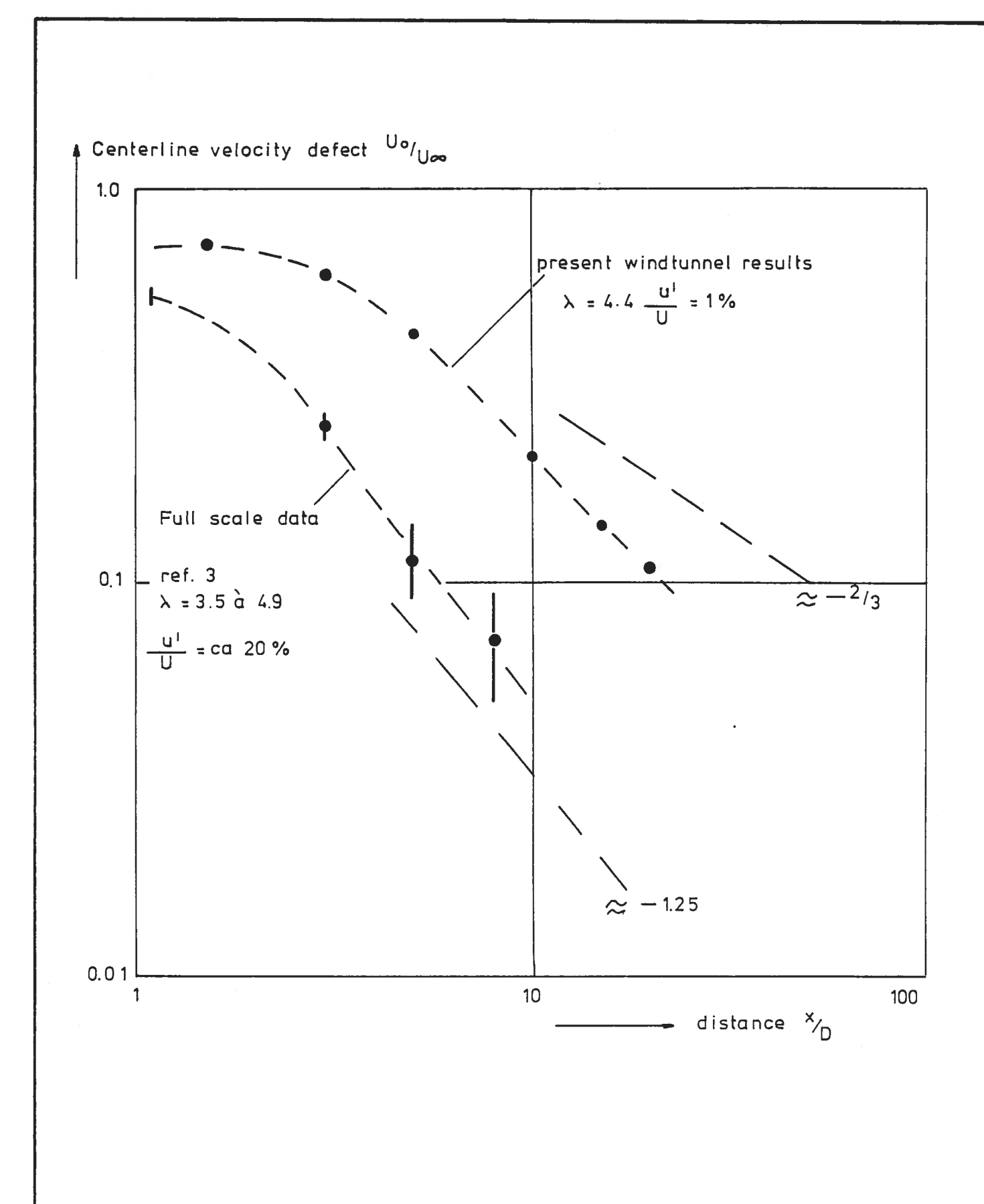
MT-TNO 8120 Fig. 10











Comparison between present and full-scale results. MT-TNO 8120 Fig. 15

